Accepted Manuscript

Novel methyl indolinone-6-carboxylates containing an indole moiety as angiokinase inhibitors

Mingze Qin, Ye Tian, Xiaoqing Sun, Simiao Yu, Juanjuan Xia, Ping Gong, Haotian Zhang, Yanfang Zhao

PII: S0223-5234(17)30634-7

DOI: 10.1016/j.ejmech.2017.08.031

Reference: EJMECH 9675

To appear in: *European Journal of Medicinal Chemistry*

Received Date: 27 May 2017

Revised Date: 11 August 2017

Accepted Date: 11 August 2017

Please cite this article as: M. Qin, Y. Tian, X. Sun, S. Yu, J. Xia, P. Gong, H. Zhang, Y. Zhao, Novel methyl indolinone-6-carboxylates containing an indole moiety as angiokinase inhibitors, *European Journal of Medicinal Chemistry* (2017), doi: 10.1016/j.ejmech.2017.08.031.

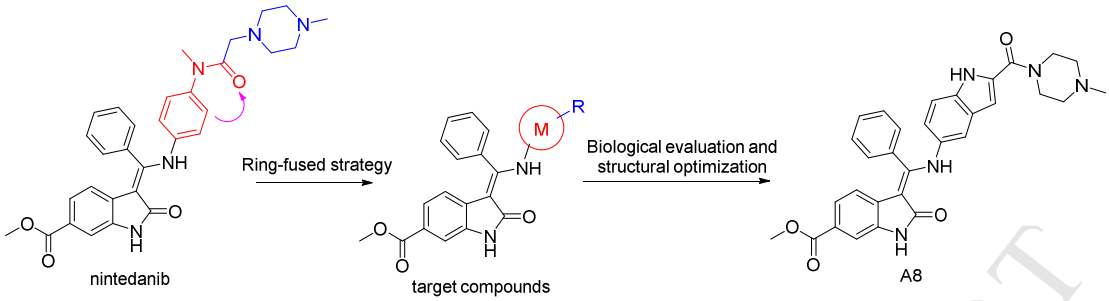

Novel methyl indolinone-6-carboxylates containing an indole moiety as angiokinase inhibitors

Mingze Qin[a], Ye Tian[a], Xiaoqing Sun[a], Simiao Yu[a], Juanjuan Xia[a], Ping Gong[a], Haotian Zhang[b,*], Yanfang Zhao[a,*]

[a] Key Laboratory of Structure-Based Drug Design and Discovery (Shenyang Pharmaceutical University), Ministry of Education, 103 Wenhua Road, Shenyang 110016, PR China
[b] Department of Pharmacology, Shenyang Pharmaceutical University, 103 Wenhua Road, Shenyang 110016, PR China

∗ Corresponding author.
Tel: +86 24 2398 6282; Fax: +86 24 2398 6282;
E-mail address: yanfangzhao@126.com (Y. Zhao); zhanghaotian2087@163.com (H. Zhang)

Abstract

A novel series of methyl indolinone-6-carboxylates bearing an indole moiety were identified as potent angiokinase inhibitors. The most active compound, **A8**, potently targeted the kinase activities of vascular endothelial growth factor receptors 2 and 3, and platelet-derived growth factor receptors α and β, with IC_{50} values in the nanomolar range. In addition, **A8** effectively suppressed the proliferation of human umbilical vein endothelial cells, and HT-29 and MCF-7 cancer cells, by inducing apoptosis. Compound **A8** is thus a promising candidate for further investigation.

Keywords: methyl indolinone-6-carboxylates; ring-fused strategy; angiokinase inhibitors; antitumour activity

1. Introduction

Angiogenesis is critical to the growth of solid tumours, and is regulated by a complex balance among several endogenous molecules [1,2]. Vascular endothelial growth factor (VEGF) directly stimulates endothelial cell proliferation and vascular permeability by binding to its cognate receptor (VEGFR). Thus, VEGF acts as a highly potent proangiogenic factor [3,4]. In addition, several studies have elucidated indispensable roles of platelet-derived growth factor (PDGF) and its cognate receptor (PDGFR) during angiogenesis. These molecules regulate the recruitment of pericytes, which are required for blood vessel formation and stabilization [5,6].

Inhibiting tumour angiogenesis by simultaneously targeting the VEGFR and PDGFR has been proven to provide a successful therapeutic approach [7–9]. The indolinone scaffold facilitates a suitable chemical interaction with the hinge region of the VEGFR and PDGFR, whereby the lactam group interacts with the protein backbone *via* two pivotal hydrogen bonds [10]. A large number of bioactive indolinones have been reported by different groups [11–13]. Nintedanib, a potent indolinone-based compound, has just been approved for clinical use in patients with non-small cell lung cancer or idiopathic pulmonary fibrosis [14]. In addition to targeting angiokinases within the VEGFR and PDGFR families with high affinity, this compound also inhibits the activity of the fibroblast growth factor receptor (FGFR), which is involved in the "angiogenic switch" response to sustained blockade of VEGF signalling [15].

Here, we reported the discovery of a series of indolinones bearing an indole moiety that act as potent angiokinase inhibitors (Fig. 1). Detailed structure-activity relationship studies were conducted and led to the identification of compound **A8**. The results of our biological evaluations clearly demonstrated that **A8** potently inhibited the activities of angiokinases including VEGFR-2, VEGFR-3, PDGFRα and PDGFRβ. In addition, **A8** inhibited the proliferation of human umbilical vein endothelial cells (HUVECs), as well as cancer cell lines such as HT-29 and MCF-7, by inducing apoptosis.

(Insert **Figure 1** here)

2. Results and discussion

2.1. Chemistry

The preparation of compounds **A1–A4** is described in Scheme 1. Intermolecular cyclisation of 2-amino-5-nitrophenol (**1**) with chloroacetyl chloride afforded benzoxazole intermediate **2** [18], which was readily converted to amines **3a** and **3b** *via* sequential nucleophilic substitution and hydrogenation reactions in a one-pot manner. The benzimidazole intermediates **6a** and **6b** were prepared using a similar method, except that N^1-methyl-4-nitrobenzene-1,2-diamine (**4**) was used as the starting material. Compounds **A1–A4** were generated by condensation of the corresponding amine (**3a**, **3b**, **6a** and **6b**) with commercially available methyl (*E*)-3-(methoxy(phenyl)methylene)-2-oxoindoline-6-carboxylate (**15**) in an addition-elimination sequence.

(Insert **Scheme** 1 here)

The synthesis of compounds **A5–A17** is outlined in Scheme 2. Amidation of

5-nitro-1*H*-indole-2-carboxylic acid (**7**) with secondary amines gave rise to the desired intermediates (**8a** and **8b**). Intermediate **8b** underwent an *N*-alkylation reaction and readily converted to **8c** and **8d**, respectively, *via* a S_N2 mechanism [19]. The selective reduction of the amide groups of **8a** and **8b** using borane afforded **9a** and **9b**, which were further hydrogenated to provide amines **10a** and **10b**, respectively. Alternatively, intermediates **8a–d** were readily converted to the corresponding amines **11a–d** under standard hydrogenation conditions. On the other hand, 5-nitro-1*H*-indole (**12**) was converted to Mannich bases **13a**, **13e** and **13g** *via* a classical Mannich reaction mechanism [16,20]. The **13b**, **13c**, **13d** and **13f** intermediates were obtained when **13a** and **13e** were reacted with suitable alkylating reagents. Intermediates **14a–g** were generated when **13a–g** were exposed to hydrogen. Reaction of these amines (**10a**, **10b**, **11a–d** and **14a–g**) with intermediate **15** generated the desired compounds, **A5–A17**.

(Insert **Scheme** 2 here)

2.2. Biological evaluation

*2.2.1. Discovery of indole-containing compounds **A5** and **A6***

The binding mode of nintedanib at the ATP-binding site of VEGFR-2 has been confirmed [10]. The methyl indolinone-6-carboxylate scaffold formed three hydrogen bonds to Cys^{919}, Glu^{917} and Lys^{868} in the hinge region, providing high-affinity binding to this kinase. Furthermore, the methyl piperazinyl group was oriented to the solvent region, and the nitrogen atom of this moiety interacted with Glu^{850} *via* a bidentate ionic bond. Based on these observations, we conducted a programme of structure-based modifications of the chemical structure of nintedanib, in an attempt to identify potent analogues. At the beginning of our study, a ring-fused strategy was applied to build a bicyclic fragment. Furthermore, previous reports by Roth *et al.* and ourselves [14,17] indicated that dimethylamine and methyl piperazinyl groups might provide optimal substitutions, and compounds **A1–A6**, which contained benzoxazole, benzimidazole and indole moieties, respectively, were therefore synthesized as proof-of-concept compounds.

First, the effects of compounds **A1–A6** on the enzymatic activities of VEGFR-2 and PDGFRβ were evaluated. As shown in Table 1, the benzoxazole derivative **A2** exhibited moderate inhibitory activity, whereas **A1** was completely inactive at a concentration of 1 μM, indicating that the benzoxazole fragment was not well tolerated. In contrast, the benzimidazole and indole derivatives (**A3–A6**) displayed promising effects on enzymatic activity. Benzimidazoles **A3** and **A4** produced effective inhibition of PDGFRβ, with 50% inhibitory concentrations (IC_{50}) of 45.5 and 61 nM, respectively. However, both compounds were less active against VEGFR-2 (IC_{50}: 384.7 and 257.2 nM, respectively). Compounds with an indole moiety (**A5** and **A6**) exhibited significantly greater inhibition of VEGFR-2 (IC_{50}: 138.3 and 106.1 nM, respectively), and provided suitable starting points for further optimization.

(Insert **Table 1** here)

To explore the potential of these compounds further, they were screened for antiproliferative activity in selected human cancer cell lines, which included A549

(human non-small cell lung cancer), MCF-7 (human breast cancer) and HT-29 (human colon cancer) cells. These findings demonstrated that both benzoxazoles (**A1** and **A2**) were inactive at the cellular level, which was consistent with their weak inhibition of receptor kinase activity. Similarly, the benzimidazoles (**A3** and **A4**) exhibited weak antiproliferative activity, thereby limiting their suitability for further investigations. The indole derivatives (**A5** and **A6**) produced effective inhibition of the proliferation of the tested cancer cell lines, especially in HT-29 and MCF-7 cells. Taken together, these findings indicated that the indole moiety may be suitable for this region, and detailed modifications could be conducted to increase potency further.

2.2.2. Modifications of indole precursors

Previous findings [10] indicated that a rational orientation of the amino group, which facilitated an ionic interaction with Glu^{850}, was crucial for activity. Compounds **A11**, **A15** and **A17** were prepared by shifting the aminomethyl group at the 2-position of indole to the 3-position, with the aim of evaluating the influence of this structural change on activity. However, these compounds exhibited sharply reduced inhibition of VEGFR-2. Notably, replacing the dimethylamino and piperazinyl groups with a morpholino fragment resulted in a loss of potency. Compounds **A11** and **A15** suppressed PDGFRβ activity with IC_{50} values of 60.7 and 135.1 nM, respectively, whereas the corresponding value for **A17** was 241.6 nM. These results were consistent with our previous findings [17], which indicated that a dimethylamino or piperazinyl group was preferred.

(Insert **Table 2** here)

The promising activity of **A11** as an inhibitor of PDGFRβ led to the preparation of more derivatives *via N*-alkylation of the indole, with the intention of improving potency. Although this approach generally failed to identify potent compounds, some valuable results were obtained. As compared with the **A11** precursor (IC_{50} for VEGFR-2 > 1000 nM; IC_{50} for PDGFRβ = 60.7 nM), the introduction of methyl (**A12**; IC_{50} for VEGFR-2 = 808.5 nM; IC_{50} for PDGFRβ = 64.6 nM), ethyl (**A13**; IC_{50} for VEGFR-2 = 431.2 nM; IC_{50} for PDGFRβ = 34.3 nM) or isopropyl (**A14**; IC_{50} for VEGFR-2 = 646.5 nM; IC_{50} for PDGFRβ = 49.2 nM) groups did not offer any significant advantage with respect to the inhibition of enzymatic activity. Notably, some of these derivatives (**A11**, **A12** and **A14**) effectively suppressed the proliferation of HT-29 cells with IC_{50} values of 0.13, 0.46 and 0.25 μM, respectively, which suggested the involvement of other biological targets beyond those examined in the current study. The biological results demonstrated that the amino group linked to the 3-position of indole was not well tolerated. As a consequence, research focus returned to the 2-substituted indole scaffold.

The methylene linker between the amino group and indole was replaced by an amide unit, and this generated compounds **A7** and **A8**. Interestingly, these two compounds produced different results. Compound **A7**, with a dimethylamino group, was completely inactive in the enzymatic assay. However, compound **A8**, bearing a piperazinyl group, was very active, with IC_{50} values of 69.1 and 22 nM for VEGFR-2 and PDGFRβ activities, respectively. Based on these observations, minor modifications were made at the indole nitrogen atom, which produced the alkylated

derivatives, **A9** and **A10**. Both of these compounds exhibited slightly reduced potency with respect to VEGFR-2 and PDGFRβ inhibition, as compared to **A8**. Interestingly, the effective inhibition of enzymatic activity by **A8** translated to potent antiproliferative activity against cancer cell lines. This compound suppressed the growth of A549, MCF-7 and HT-29 cells, with IC_{50} values of 2.99, 1.56 and 1.17 μM, respectively. To exclude the effect of cytotoxicity, **A8** was evaluated for inhibitory activity against normal cells derived from human embryonic kidney (HEK293T). However, no significant inhibition of proliferation was observed for treatment with 10 μM **A8** (Figure S1). Taken together, these findings identified compound **A8** as a promising candidate for subsequent biological assessment.

2.2.3. Analysis of apoptosis

To determine whether compound **A8** inhibited the proliferation of cancer cells by inducing apoptosis, a biparametric cytofluorimetric analysis using propidium iodide and annexin V-fluorescein isothiocyanate staining was conducted in HT-29 and MCF-7 cells. In addition, human umbilical vein endothelial cells (HUVECs) were employed to further evaluate the effect of **A8** on angiogenesis. These cell lines were treated with **A8** at different concentrations (0, 0.3, 1 and 3 μM) for 48 h prior to staining and analysis by flow cytometry. As shown in Figure 2, the apoptosis rate in HUVECs was significantly elevated from 7.57% (control) to 81.57% in the presence of 1 μM **A8**. When the cells were treated with 3 μM **A8**, the apoptosis rate reached 95.28%, which indicated that **A8** induced apoptosis of HUVECs in a concentration-dependent manner. Severe **A8**-triggered apoptosis was also observed in HT-29 and MCF-7 cells (Figure 2).

(Insert **Figure 2** here)

2.2.4. Inhibitory activity against selected angiokinases

In an attempt to investigate the effects of compound **A8** on a range of angiokinases, we evaluated its inhibitory activities against VEGFR-3, PDGFRα and FGFR1. As shown in Table 3, **A8** produced strong inhibition of VEGFR-3 (IC_{50} = 18.2 nM) and PDGFRα (IC_{50} = 4.4 nM), and moderate activity against FGFR1 (IC_{50} = 1507 nM). These biological results clearly demonstrated that compound **A8** was a potent inhibitor of several angiokinases.

(Insert **Table 3** here)

2.3. Molecular docking study

To elucidate the favorable VEGFR-2 inhibition of **A8**, a detailed docking analysis was conducted using AutoDock 4.2. The binding conformations were analyzed using Discovery Studio Visualizer 4.0. The X-ray structure of the kinase domain of VEGFR-2 was obtained from the Protein Data Bank (PDB code: 3C7Q). Figure 3 showed the binding model overlay of compound **A8** with nintedanib, which suggested that the two compounds acted in a similar way. Also as shown in Figure 3, **A8** formed three hydrogen bonds with Cys^{919}, Glu^{917} and Lys^{868} in the hinge region. Furthermore, the nitrogen atom of the piperazinyl group interacted with Glu^{850} *via* a bidentate ionic bond. The docking results indicated that compound **A8** fitted well to the kinase domain of VEGFR-2.

(Insert **Figure 3** here)

3. Conclusions

In summary, a novel series of indolinone derivatives containing an indole moiety were identified as potent angiokinase inhibitors. Biological optimization led to the identification of **A8**, which potently inhibited the activities of VEGFR-2, VEGFR-3, PDGFRα and PDGFRβ with IC_{50} values of 69.1, 18.2, 4.4 and 22 nM, respectively. Although the overall inhibitory activity of **A8** was slightly less than that of nintedanib, its novel chemical structure provides a promising candidate for further development. In addition, compound **A8** effectively suppressed the proliferation of HUVECs and HT-29 and MCF-7 cancer cells by inducing apoptosis. Further investigations on the pharmacokinetics and *in vivo* activity of **A8** are underway.

4. Experimental section

4.1. Chemistry

Reagents and solvents were obtained from commercial sources and used without further purification. All the reactions were monitored by TLC using silica gel GF/UV 254. Flash chromatography was performed using silica gel (300–400 mesh). The purity of the synthesized compounds was measured by high performance liquid chromatography (HPLC, Agilent, USA), and was confirmed to be higher than 95%. Melting points were determined on a Büchi Melting Point B-540 apparatus (Büchi Labortechnik, Flawil, Switzerland). The ^{1}H and ^{13}C NMR spectra were recorded on Bruker AV-400 spectrometer, with TMS as an internal standard. The low resolution of ESI-MS was recorded on an Agilent 1100 LC-MS spectrometer, and high resolution mass spectrometry was performed on an Agilent Accurate-Mass Q-TOF 6530 in ESI mode.

*4.1.1. 2-(Chloromethyl)-6-nitrobenzo[d]oxazole (**2**)*

To a solution of intermediate **1** (4.93 g, 0.032 mol) in chlorobenzene (30 mL) was added chloroacetyl chloride (4.03 g, 0.036 mol) dropwise at 0 °C, followed by addition of pyridine (0.13 g, 1.6 mmol). Stirring was continued for 1 h at room temperature. Subsequently, *p*-toluenesulfonic acid (0.55 g, 3.2 mmol) was added, the mixture was stirred for another 8 h under reflux. The precipitate was filtered off, the filtrate was washed with brine. The solvent was concentrated to give a residue, which was triturated with ethanol to give intermediate **2** (4.76 g, 70.2%) as a yellow solid. ^{1}H NMR (400 MHz, DMSO-d_6) δ 6.48 (d, J = 8.3 Hz,1H, ArH), 6.27 (d, J = 2.5 Hz, 1H, ArH), 6.04 (dd, J = 8.3, 2.6 Hz, 1H, ArH), 4.24 (s, 2H, CH_2). ESI-MS m/z: 213.0 $[M+H]^+$.

*4.1.2. 2-(Chloromethyl)-1-methyl-5-nitro-1H-benzo[d]imidazole (**5**)*

To a solution of intermediate **4** (2 g, 12 mmol) and triethylamine (1.34 g, 13.2 mmol) in ethyl acetate (10 mL) was added chloroacetyl chloride (1.48 g, 13.2 mmol) dropwise at 0 °C. The mixture was stirred for 30 min at room temperature, then acetic acid (0.5 mL) was added. Stirring was maintained for 20 h under reflux. After that time, the solution was cooled down. The precipitate was filtered off to give a crude product, which was recrystallized from ethyl acetate to give **5** (1.85 g, 68.5%) as a yellow solid. ESI-MS m/z: 226.1 $[M+H]^+$.

*4.1.3. General procedure for preparation of intermediates **3a**, **3b**, **6a**, and **6b***

To a solution of an intermediate (**2** or **5**, 4.7 mmol) and appropriate amine (4.7

mmol) in dichloromethane (5 mL) was added *N*,*N*-diisopropylethylamine (5.5 mmol). The mixture was stirred at 30 °C for 8–12 h until TLC showed the completion of the reaction. The solution was diluted with ethanol (20 mL), and palladium on charcoal (10% w/w) was added. The reaction mixture was hydrogenated at room temperature for 5 h. After that time, the catalyst was filtered off and the filtrate was evaporated. The residue was purified by column chromatography (CH_2Cl_2/MeOH, 100/1 to 30/1) to generate the desired intermediates.

*4.1.3.1. 2-((Dimethylamino)methyl)benzo[d]oxazol-6-amine (**3a**).* Gray solid. Yield: 67%. ^{1}H NMR (400 MHz, DMSO-d_6) δ 6.61 (d, *J* = 8.1 Hz, 1H, ArH), 6.14–6.00 (m, 2H, ArH), 4.72 (s, 2H, NH_2), 4.60 (s, 2H, CH_2), 2.90 (s, 6H, CH_3). ESI-MS m/z: 192.1 $[M+H]^+$.

*4.1.3.2. 2-((4-Methylpiperazin-1-yl)methyl)benzo[d]oxazol-6-amine (**3b**).* Gray solid. Yield: 70%. ESI-MS m/z: 247.2 $[M+H]^+$.

*4.1.3.3. 2-((Dimethylamino)methyl)-1-methyl-1H-benzo[d]imidazol-5-amine (**6a**).* Gray solid. Yield: 62%. ^{1}H NMR (400 MHz, DMSO-d_6) δ 7.15 (d, *J* = 8.5 Hz, 1H, ArH), 6.72 (d, *J* = 1.8 Hz, 1H, ArH), 6.58 (dd, *J* = 8.5, 2.0 Hz, 1H, ArH), 4.86 (s, 2H, NH_2), 3.70 (s, 3H, $NC\underline{H}_3$), 3.61 (s, 2H, CH_2), 2.20 (s, 6H, $N(C\underline{H}_3)_2$). ESI-MS m/z: 205.1 $[M+H]^+$.

*4.1.3.4. 1-Methyl-2-((4-methylpiperazin-1-yl)methyl)-1H-benzo[d]imidazol-5-amine (**6b**).* Gray solid. Yield: 77%. ^{1}H NMR (400 MHz, DMSO-d_6) δ 7.17 (d, *J* = 8.5 Hz, 1H, ArH), 6.72 (s, 1H, ArH), 6.59 (dd, *J* = 8.5, 1.6 Hz, 1H, ArH), 3.88 (s, 2H, NH_2), 3.73 (s, 2H, CH_2), 3.71 (s, 3H, CH_3), 2.78 (s, 4H, piperazinyl), 2.57 (s, 4H, piperazinyl), 2.48 (s, 3H, CH_3). ESI-MS m/z: 260.2 $[M+H]^+$.

*4.1.4. General procedure for preparation of intermediates **8a** and **8b***

To a solution of intermediate **7** (10 mmol), appropriate amine (30 mmol), and HATU (30 mmol) in DMF (15 mL) was added *N*,*N*-diisopropylethylamine (30 mmol) slowly. The mixture was stirred at room temperature for 12 h. When TLC showed the completion of the reaction, the solution was poured into water. The precipitate was filtered off to give the desired intermediates.

*4.1.4.1. N,N-dimethyl-5-nitro-1H-indole-2-carboxamide (**8a**).* Orange solid. Yield: 72%. ESI-MS m/z: 234.1 $[M+H]^+$.

*4.1.4.2. (4-Methylpiperazin-1-yl)(5-nitro-1H-indol-2-yl)methanone (**8b**).* Yellow solid. Yield: 63%. ESI-MS m/z: 289.1 $[M+H]^+$.

*4.1.5. General procedure for preparation of intermediates **8c** and **8d***

To a solution of intermediate **8b** (1 mmol) in dichloromethane was added sodium hydride (2 mmol) at 0 °C. Stirring was continued for 30 min. After that time, appropriate alkyl halide (1.5 mmol) in dichloromethane was added dropwise. The mixture was stirred at room temperature for 3–6 h until TLC indicated the completion of the reaction. The reaction was quenched with aqueous NH_4Cl. The organic phase was washed with water, and was concentrated to give a residue, which was purified by column chromatography (CH_2Cl_2/MeOH, 100/1 to 75/1) to afford the target compounds.

*4.1.5.1. (1-Methyl-5-nitro-1H-indol-2-yl)(4-methylpiperazin-1-yl)methanone (**8c**).* Light yellow solid. Yield: 57%. ESI-MS m/z: 303.1 $[M+H]^+$.

*4.1.5.2. (1-Ethyl-5-nitro-1H-indol-2-yl)(4-methylpiperazin-1-yl)methanone (**8d**).* Light yellow solid. Yield: 60%. ESI-MS m/z: 317.1 $[M+H]^+$.

*4.1.6. General procedure for preparation of intermediates **9a** and **9b***

To a solution of intermediate (**8a** and **8b**, 6.4 mmol) in THF (10 mL) was added borane dimethyl sulphide complex (2M solution in THF, 19 mL) at room temperature. The reaction mixture was heated at reflux for 1 h. To the mixture was added 6M HCl dropwise and stirred under reflux for a further 30 minutes. The reaction mixture was cooled to room temperature, when 4N NaOH solution was added. The mixture was extracted with dichloromethane, and washed with brine. The organic layer was concentrated to give the crude product, which was purified by column chromatography (CH_2Cl_2/MeOH, 100/1 to 80/1) to afford the desired intermediate.

*4.1.6.1. N,N-dimethyl-1-(5-nitro-1H-indol-2-yl)methanamine (**9a**).* Yellow solid. Yield: 63%. ESI-MS m/z: 220.1 $[M+H]^+$.

*4.1.6.2. 2-((4-Methylpiperazin-1-yl)methyl)-5-nitro-1H-indole (**9b**).* Yellow solid. Yield: 72%. ESI-MS m/z: 275.2 $[M+H]^+$.

*4.1.7. General procedure for preparation of intermediates **10a** and **10b***

At room temperature, palladium on charcoal (10% w/w) was added to a solution of intermediates (**9a** and **9b**, 1.8 mmol) in ethanol. The reaction mixture was hydrogenated for 6 h. When TLC showed the completion of the reaction, the catalyst was filtered off. The filtrate was evaporated to give the desired intermediates.

*4.1.7.1. 2-((Dimethylamino)methyl)-1H-indol-5-amine (**10a**).* Yellow solid. Yield: 81%. ^{1}H NMR (400 MHz, DMSO-d_6) δ 10.54 (s, 1H, NH), 7.01 (d, *J* = 8.4 Hz, 1H, ArH), 6.61 (d, *J* = 1.0 Hz, 1H, ArH), 6.44 (dd, *J* = 8.5, 1.8 Hz, 1H, ArH), 6.02 (s, 1H, ArH), 5.10 (s, 2H, NH_2), 3.57 (s, 2H, CH_2), 2.24 (s, 6H, CH_3). ESI-MS m/z: 190.1 $[M+H]^+$.

*4.1.7.2. 2-((4-Methylpiperazin-1-yl)methyl)-1H-indol-5-amine (**10b**).* Yellow solid. Yield: 66%. ^{1}H NMR (400 MHz, DMSO-d_6) δ 10.45 (s, 1H, NH), 6.99 (d, *J* = 8.4 Hz, 1H, ArH), 6.58 (s, 1H, ArH), 6.41 (d, *J* = 8.0 Hz, 1H, ArH), 5.96 (s, 1H, ArH), 4.64 (s, 2H, NH_2), 3.48 (s, 2H, CH_2), 2.33 (br, 8H, piperazinyl), 2.14 (s, 3H, CH_3). ESI-MS m/z: 245.2 $[M+H]^+$.

*4.1.8. General procedure for preparation of intermediates **11a–11d***

Intermediates **11a–11d** were prepared according to the synthetic method as described for intermediates **10a** and **10b** by using intermediate **8a–8d** as the reactants.

*4.1.8.1. 5-Amino-N,N-dimethyl-1H-indole-2-carboxamide (**11a**).* Yellow solid. Yield: 42%. ESI-MS m/z: 204.1 $[M+H]^+$.

*4.1.8.2. (5-Amino-1H-indol-2-yl)(4-methylpiperazin-1-yl)methanone (**11b**).* Yellow solid. Yield: 53%. ESI-MS m/z: 259.2 $[M+H]^+$.

*4.1.8.3. (5-Amino-1-methyl-1H-indol-2-yl)(4-methylpiperazin-1-yl)methanone (**11c**).* Yellow solid. Yield: 68%. ESI-MS m/z: 273.2 $[M+H]^+$.

*4.1.8.4. (5-Amino-1-ethyl-1H-indol-2-yl)(4-methylpiperazin-1-yl)methanone (**11d**).* Yellow solid. Yield:70%. ESI-MS m/z: 287.2 $[M+H]^+$.

*4.1.9. General procedure for preparation of intermediates **13a**, **13e**, and **13g***

To a mixture of intermediate **12** (6.2 mmol), paraformaldehyde (9.3 mmol) in acetic acid (5 mL) was added appropriate secondary amine (9.3 mmol). The mixture

was stirred at 35 °C for 5–8 h and was monitored by TLC. The solution was alkalized with aqueous NaOH to pH 8–9, and was extracted with dichloromethane. The organic phase was concentrated to give a residue, which was purified by column chromatography (CH_2Cl_2/MeOH, 100/1 to 75/1) to provide the desired intermediates.

*4.1.9.1. N,N-dimethyl-1-(5-nitro-1H-indol-3-yl)methanamine (**13a**).* Yellow solid. Yield: 42%. ESI-MS m/z: 220.1 $[M+H]^+$.

*4.1.9.2. 3-((4-Methylpiperazin-1-yl)methyl)-5-nitro-1H-indole (**13e**).* Yellow solid. Yield: 51%. ESI-MS m/z: 275.2 $[M+H]^+$.

*4.1.9.3. 4-((5-Nitro-1H-indol-3-yl)methyl)morpholine (**13g**).* Yellow solid. Yield: 56%. ESI-MS m/z: 262.1 $[M+H]^+$.

*4.1.10. General procedure for preparation of intermediates **13b–13d** and **13f***

Intermediates **13b–13d** and **13f** were prepared according to the synthetic method as described for intermediates **8c** and **8d** by using intermediate **13a** and **13e** as the reactants. The crude product was purified by silica gel column chromatography eluting with CH_2Cl_2/MeOH (120/1 to 70/1).

4.1.10.1. N,N-dimethyl-1-(1-methyl-5-nitro-1*H*-indol-3-yl)methanamine (**13b**). Yellow solid. Yield: 67%. ESI-MS m/z: 234.1 $[M+H]^+$.

*4.1.10.2. 1-(1-Ethyl-5-nitro-1H-indol-3-yl)-N,N-dimethylmethanamine (**13c**).* Yellow solid. Yield: 62%. ESI-MS m/z: 248.1 $[M+H]^+$.

*4.1.10.3. 1-(1-Isopropyl-5-nitro-1H-indol-3-yl)-N,N-dimethylmethanamine (**13d**).* Yellow solid. Yield: 76%. ESI-MS m/z: 262.1 $[M+H]^+$.

*4.1.10.4. 1-Methyl-3-((4-methylpiperazin-1-yl)methyl)-5-nitro-1H-indole (**13f**).* Yellow solid. Yield: 57%. ESI-MS m/z: 289.2 $[M+H]^+$.

*4.1.11. General procedure for preparation of intermediates **14a–14g***

Intermediates **14a–14g** were prepared according to the synthetic method as described for intermediates **10a** and **10b** by using intermediate **13a–13g** as the reactants. The crude product was purified by silica gel column chromatography eluting with CH_2Cl_2/MeOH (100/1 to 60/1) to afford **14a–14g**, respectively.

*4.1.11.1. 3-((Dimethylamino)methyl)-1H-indol-5-amine (**14a**).* Brown solid. Yield: 46%. ^{1}H NMR (400 MHz, DMSO-d_6) δ 10.40 (s, 1H, NH), 7.02 (d, J = 9.4 Hz, 2H, ArH), 6.75 (s, 1H, ArH), 6.46 (dd, J = 8.3, 1.5 Hz, 1H, ArH), 4.48 (s, 2H, NH_2), 3.42 (s, 2H, CH_2), 2.13 (s, 6H, CH_3). ESI-MS m/z: 190.1 $[M+H]^+$.

*4.1.11.2. 3-((Dimethylamino)methyl)-1-methyl-1H-indol-5-amine (**14b**).* Brown solid. Yield: 69%. ESI-MS m/z: 204.1 $[M+H]^+$.

*4.1.11.3. 3-((Dimethylamino)methyl)-1-ethyl-1H-indol-5-amine (**14c**).* Brown oil. Yield: 72%. ESI-MS m/z: 218.1 $[M+H]^+$.

*4.1.11.4. 3-((Dimethylamino)methyl)-1-isopropyl-1H-indol-5-amine (**14d**).* Yellow solid. Yield: 57%. ESI-MS m/z: 232.2 $[M+H]^+$.

*4.1.11.5. 3-((4-Methylpiperazin-1-yl)methyl)-1H-indol-5-amine (**14e**).* Brown solid. Yield: 57%. ^{1}H NMR (400 MHz, DMSO-d_6) δ 10.46 (s, 1H, NH), 7.03 (d, J = 8.2 Hz, 2H, ArH), 6.74 (d, J = 1.8 Hz, 1H, ArH), 6.47 (dd, J = 8.4, 1.7 Hz, 1H, ArH), 3.53 (s, 2H, CH_2), 2.36 (m, J = 23.9 Hz, 7H, piperazinyl, CH_3), 2.19 (s, 4H, piperazinyl). ESI-MS m/z: 245.2 $[M+H]^+$.

*4.1.11.6. 1-Methyl-3-((4-methylpiperazin-1-yl)methyl)-1H-indol-5-amine (**14f**).*

Yellow solid. Yield: 66%. ESI-MS m/z: 259.2 $[M+H]^+$.

*4.1.11.7. 3-(Morpholinomethyl)-1H-indol-5-amine (**14g**).* Yellow solid. Yield: 57%. ^{1}H NMR (400 MHz, DMSO-d_6) δ 10.51 (s, 1H, NH), 7.03 (d, *J* = 8.4 Hz, 2H, ArH), 6.76 (d, *J* = 1.8 Hz, 1H, ArH), 6.46 (d, *J* = 10.5 Hz, 1H, ArH), 4.45 (s, 2H, NH_2), 3.60–3.50 (t, 4H, morpholinyl), 3.47 (s, 2H, CH_2), 2.34 (s, 4H, morpholinyl). ESI-MS m/z: 232.1 $[M+H]^+$.

*4.1.12. General procedure for preparation of compounds **A1–A17**.*

A mixture of intermediate (**3a**, **3b**, **6a**, **6b**, **10a**, **10b**, **11a–d**, and **14a–g**, 1.5 mmol) and methyl (*E*)-3-(methoxy(phenyl)methylene)-2-oxoindoline-6-carboxylate (1.5 mmol) in methanol (10 mL) was stirred under reflux for 5–10 h. When TLC showed the completion of the reaction, the solution was cooled to room temperature. The precipitate was filtered off to give a crude product, which was recrystallized from methanol to provide the target compounds.

*4.1.12.1. Methyl (Z)-3-(((2-((dimethylamino)methyl)benzo[d]oxazol-6-yl)amino)(phenyl)methylene)-2-oxoindoline-6-carboxylate (**A1**).* Yellow solid. Yield: 42%. Mp: 298.2–301.7 °C. ^{1}H NMR (400 MHz, DMSO-d_6) δ 12.18 (s, 1H, NH), 10.92 (s, 1H, NH), 7.63–7.54 (m, 3H, ArH), 7.48 (dd, *J* = 7.7, 1.4 Hz, 2H, ArH), 7.41 (d, *J* = 1.3 Hz, 1H, ArH), 7.18 (dd, *J* = 8.2, 1.5 Hz, 1H, ArH), 6.67 (d, *J* = 8.3 Hz, 1H, ArH), 6.41 (dd, *J* = 8.4, 2.4 Hz, 1H, ArH), 6.27 (d, *J* = 2.4 Hz, 1H, ArH), 5.78 (d, *J* = 8.2 Hz, 1H, ArH), 4.66 (s, 2H, CH_2), 3.76 (s, 3H, OCH_3), 2.95 (s, 6H, CH_3). ^{13}C NMR (101 MHz, DMSO-d_6) δ 170.60, 166.93, 159.24, 156.11, 144.40, 136.30, 133.69, 132.77, 132.51, 130.74, 129.86, 129.67, 128.80, 123.94, 123.38, 121.84, 117.91, 117.36, 110.33, 109.83, 96.95, 60.48, 56.49, 52.21. HRMS (ESI) for $C_{27}H_{24}N_4O_4$ $[M + H]^+$, calcd: 469.1870, found: 469.1873.

*4.1.12.2. Methyl (Z)-3-(((2-((4-methylpiperazin-1-yl)methyl)benzo[d]oxazol-6-yl)amino)(phenyl)methylene)-2-oxoindoline-6-carboxylate (**A2**).* Yellow solid. Yield: 53%. Mp: 310.8–314.0 °C. ^{1}H NMR (400 MHz, DMSO-d_6) δ 12.16 (s, 1H, NH), 10.92 (s, 1H, NH), 7.56 (m, *J* = 11.0, 4.8 Hz, 3H, ArH), 7.48 (d, *J* = 6.5 Hz, 2H, ArH), 7.41 (d, *J* = 1.0 Hz, 1H, ArH), 7.18 (dd, *J* = 8.3, 1.3 Hz, 1H, ArH), 6.72 (d, *J* = 8.3 Hz, 1H, ArH), 6.45 (dd, *J* = 8.4, 2.2 Hz, 1H, ArH), 6.31 (d, *J* = 2.2 Hz, 1H, ArH), 5.79 (d, *J* = 8.2 Hz, 1H, ArH), 4.69 (s, 2H, CH_2), 3.77 (s, 3H, OCH_3), 3.44 (m, *J* = 6.7, 3.8 Hz, 4H, piperazinyl), 2.90 (m, *J* = 12.8 Hz, 4H, piperazinyl), 2.59 (s, 3H, CH_3). ^{13}C NMR (101 MHz, DMSO-d_6) δ 170.61, 166.91, 159.14, 154.88, 144.58, 136.41, 133.76, 132.71, 132.31, 130.79, 129.88, 129.59, 128.83, 124.12, 123.96, 121.88, 118.00, 117.47, 110.49, 109.87, 97.24, 60.41, 56.49, 52.86, 52.24, 41.78, 19.02. HRMS (ESI) for $C_{30}H_{29}N_5O_4$ $[M + H]^+$, calcd: 524.2292, found: 524.2287.

*4.1.12.3. Methyl (Z)-3-(((2-((dimethylamino)methyl)-1-methyl-1H-benzo[d]imidazol-5-yl)amino)(phenyl)methylene)-2-oxoindoline-6-carboxylate (**A3**).* Yellow solid. Yield: 37%. Mp: 304.3–307.1 °C. ^{1}H NMR (400 MHz, DMSO-d_6) δ 12.29 (s, 1H, NH), 10.93 (s, 1H, NH), 7.54–7.47 (m, 5H, ArH), 7.42 (d, *J* = 1.2 Hz, 1H, ArH), 7.35 (d, *J* = 8.6 Hz, 1H, ArH), 7.18 (dd, *J* = 8.2, 1.4 Hz, 1H, ArH), 7.15 (d, *J* = 1.6 Hz, 1H, ArH), 6.93 (dd, *J* =

8.6, 1.8 Hz, 1H, ArH), 5.76 (d, *J* = 8.2 Hz, 1H, ArH), 3.77 (s, 3H, OCH_3), 3.74 (s, 3H, CH_3), 3.60 (s, 2H, CH_2), 2.16 (s, 6H, CH_3). ^{13}C NMR (101 MHz, DMSO-d_6) δ 170.69, 166.95, 160.41, 153.68, 142.17, 136.28, 134.51, 132.78, 132.36, 130.57, 129.83, 129.74, 128.94, 123.86, 121.83, 120.05, 117.32, 115.02, 110.44, 109.80, 96.79, 56.49, 52.21, 45.64, 30.44. HRMS (ESI) for $C_{28}H_{27}N_5O_3$ $[M + H]^+$, calcd: 482.2187, found: 482.2181.

*4.1.12.4. Methyl (Z)-3-(((1-methyl-2-((4-methylpiperazin-1-yl)methyl)-1H-benzo[d]imidazol-5-yl)amino)(phenyl)methylene)-2-oxoindoline-6-carboxylate (**A4**).* Yellow solid. Yield: 60%. Mp: 188.3–192.8 °C. ^{1}H NMR (400 MHz, DMSO-d_6) δ 12.29 (s, 1H, NH), 10.93 (s, 1H, NH), 7.51 (m, *J* = 7.1, 4.3 Hz, 5H, ArH), 7.43 (s, 1H, ArH), 7.35 (d, *J* = 8.6 Hz, 1H, ArH), 7.18 (dd, *J* = 8.2, 1.0 Hz, 1H, ArH), 7.14 (d, *J* = 1.1 Hz, 1H, ArH), 6.93 (dd, *J* = 8.5, 1.5 Hz, 1H, ArH), 5.76 (d, *J* = 8.2 Hz, 1H, ArH), 3.77 (s, 3H, OCH_3), 3.75 (s, 3H, CH_3), 3.68 (s, 2H, CH_2), 2.35 (m, *J* = 36.5 Hz, 8H, piperazinyl), 2.14 (s, 3H, CH_3). ^{13}C NMR (101 MHz, DMSO-d_6) δ 170.69, 166.95, 160.39, 153.15, 142.17, 136.28, 134.52, 132.78, 132.37, 130.58, 129.82, 129.75, 128.92, 123.87, 121.84, 120.04, 117.32, 114.94, 110.46, 109.81, 96.80, 55.02, 54.89, 53.01, 52.21, 49.06, 46.05. HRMS (ESI) for $C_{31}H_{32}N_6O_3$ $[M + H]^+$, calcd: 537.2609, found: 537.2615.

*4.1.12.5. Methyl (Z)-3-(((2-((dimethylamino)methyl)-1H-indol-5-yl)amino)(phenyl)methylene)-2-oxoindoline-6-carboxylate (**A5**).* Yellow solid. Yield: 57%. Mp: 296.2.1–299.7 °C. ^{1}H NMR (600 MHz, DMSO-d_6) δ 12.28 (s, 1H, NH), 11.05 (s, 1H, NH), 10.88 (s, 1H, NH), 7.50 (m, *J* = 6.0 Hz, 2H, ArH), 7.46 (dd, *J* = 7.8, 1.8 Hz, 2H, ArH), 7.43 (d, *J* = 1.4 Hz, 1H, ArH), 7.17 (dd, *J* = 8.2, 1.6 Hz, 1H, ArH), 7.10 (d, *J* = 8.6 Hz, 1H, ArH), 7.07 (d, *J* = 1.7 Hz, 1H, ArH), 6.68 (dd, *J* = 8.6, 2.1 Hz, 1H, ArH), 6.11 (s, 1H, ArH), 5.76 (s, 2H, ArH), 3.77 (s, 3H, OCH_3), 3.47 (s, 2H, CH_2), 2.15 (s, 6H, CH_3). ^{13}C NMR (151 MHz, DMSO-d_6) δ 170.60, 170.60, 166.91, 166.91, 160.74, 160.74, 138.54, 135.97, 134.54, 132.88, 130.29, 129.89, 129.68, 129.50, 128.82, 128.09, 123.45, 121.67, 118.63, 117.01, 115.77, 111.46, 109.68, 100.89, 96.07, 56.40, 55.28, 45.24. HRMS (ESI) for $C_{28}H_{26}N_4O_3$ $[M + H]^+$, calcd: 467.2078, found: 467.2083.

*4.1.12.6. Methyl (Z)-3-(((2-((4-methylpiperazin-1-yl)methyl)-1H-indol-5-yl)amino)(phenyl)methylene)-2-oxoindoline-6-carboxylate (**A6**).* Yellow solid. Yield: 42%. Mp: 245.3–248.7 °C. ^{1}H NMR (400 MHz, DMSO-d_6) δ 12.28 (s, 1H, NH), 11.03 (s, 1H, NH), 10.91 (s, 1H, NH), 7.47 (dd, *J* = 20.4, 8.9 Hz, 6H, ArH), 7.17 (d, *J* = 8.0 Hz, 1H, ArH), 7.13–7.04 (m, 2H, ArH), 6.68 (d, *J* = 8.3 Hz, 1H, ArH), 6.12 (s, 1H, ArH), 5.78–5.69 (m, 1H, ArH), 3.77 (s, 3H, OCH_3), 3.51 (s, 2H, CH_2), 2.33 (m, 8H, piperazinyl), 2.14 (s, 3H, CH_3). ^{13}C NMR (101 MHz, DMSO-d_6) δ 170.69, 167.01, 160.86, 138.14, 136.05, 134.65, 132.95, 130.40, 129.99, 129.75, 129.61, 128.91, 128.17, 123.54, 121.76, 118.75, 117.10, 115.86, 111.58, 109.77, 101.25, 96.15, 55.49, 55.07, 53.07, 52.18, 46.18. HRMS (ESI) for $C_{31}H_{31}N_5O_3$ $[M + H]^+$, calcd: 522.2500, found: 522.2507.

*4.1.12.7. Methyl (Z)-3-(((2-(dimethylcarbamoyl)-1H-indol-5-yl)amino)(phenyl)methylene)-2-oxoindoline-6-carboxylate (**A7**).* Yellow solid. Yield: 37%. Mp: 343.2–346.0 °C. ^{1}H NMR (400

MHz, DMSO-d_6) δ 12.27 (s, 1H, NH), 11.57 (s, 1H, NH), 10.92 (s, 1H, NH), 7.56–7.44 (m, 5H, ArH), 7.42 (s, 1H, ArH), 7.22 (d, *J* = 8.5 Hz, 2H, ArH), 7.18 (d, *J* = 8.1 Hz, 1H, ArH), 6.85 (dd, *J* = 8.9, 1.1 Hz, 1H, ArH), 6.72 (s, 1H, ArH), 5.77 (d, *J* = 8.2 Hz, 1H, ArH), 3.77 (s, 3H, OCH_3), 3.26 (s, 3H, CH_3), 3.03 (s, 3H, CH_3). ^{13}C NMR (101 MHz, DMSO-d_6) δ 170.71, 166.97, 162.67, 160.69, 136.18, 134.04, 132.81, 131.92, 130.65, 130.49, 130.23, 129.88, 129.65, 128.95, 127.34, 123.73, 121.80, 117.49, 117.22, 112.72, 109.79, 105.06, 96.47, 52.20, 41.43. HRMS (ESI) for $C_{28}H_{24}N_4O_4$ $[M + H]^+$, calcd: 481.1870, found: 481.1868.

4.1.12.8. *Methyl (Z)-3-(((2-(4-methylpiperazine-1-carbonyl)-1H-indol-5-yl)amino)(phenyl)methylene)-2-oxoindoline-6-carboxylate (**A8**).* Yellow solid. Yield: 50%. Mp: 260.7–264.8 °C. ^{1}H NMR (600 MHz, DMSO-d_6) δ 12.27 (s, 1H, NH), 11.63 (s, 1H, NH), 10.90 (s, 1H, NH), 7.58–7.45 (m, 5H, ArH), 7.43 (s, 1H, ArH), 7.22 (d, *J* = 8.7 Hz, 2H, ArH), 7.18 (d, *J* = 8.0 Hz, 1H, ArH), 6.87 (d, *J* = 8.6 Hz, 1H, ArH), 6.68 (s, 1H, ArH), 5.77 (d, *J* = 8.3 Hz, 1H, ArH), 3.77 (s, 7H, OCH_3, piperazinyl), 2.66 (s, 4H, piperazinyl), 2.44 (s, 3H, CH_3). ^{13}C NMR (151 MHz, DMSO-d_6) δ 170.62, 166.88, 161.96, 160.55, 136.11, 134.21, 132.71, 130.98, 130.75, 130.41, 129.77, 129.57, 128.86, 126.98, 123.69, 121.88, 121.73, 117.34, 117.15, 112.69, 109.72, 104.75, 96.47, 53.95, 52.12, 48.97, 44.37. HRMS (ESI) for $C_{31}H_{29}N_5O_4$ $[M + H]^+$, calcd: 536.2292, found: 536.2286.

4.1.12.9. *Methyl (Z)-3-(((1-methyl-2-(4-methylpiperazine-1-carbonyl)-1H-indol-5-yl)amino)(phenyl)methylene)-2-oxoindoline-6-carboxylate (**A9**).* Yellow solid. Yield: 50%. Mp: 245.8–248.4 °C. ^{1}H NMR (600 MHz, DMSO-d_6) δ 12.28 (s, 1H, NH), 10.92 (s, 1H, NH), 7.55–7.45 (m, 5H, ArH), 7.43 (s, 1H, ArH), 7.33 (d, *J* = 8.8 Hz, 1H, ArH), 7.25 (s, 1H, ArH), 7.18 (d, *J* = 8.3 Hz, 1H, ArH), 6.87 (s, 1H, ArH), 6.49 (s, 1H, ArH), 5.77 (d, *J* = 8.2 Hz, 1H, ArH), 3.77 (s, 3H, OCH_3), 3.66 (s, 3H, CH_3), 3.59 (m, 4H, piperazinyl), 2.33 (m, 4H, piperazinyl), 2.20 (s, 3H, CH_3). HRMS (ESI) for $C_{32}H_{31}N_5O_4$ $[M + H]^+$, calcd: 550.2449, found: 550.2450.

4.1.12.10. *Methyl (Z)-3-(((1-ethyl-2-(4-methylpiperazine-1-carbonyl)-1H-indol-5-yl)amino)(phenyl)methylene)-2-oxoindoline-6-carboxylate (**A10**).* Yellow solid. Yield: 50%. Mp: 329.3–331.2 °C. ^{1}H NMR (600 MHz, DMSO-d_6) δ 12.36 (s, 1H, NH), 10.98 (s, 1H, NH), 7.60–7.53 (m, 5H, ArH), 7.49 (s, 1H, ArH), 7.43 (d, *J* = 8.8 Hz, 1H, ArH), 7.28 (s, 1H, ArH), 7.24 (d, *J* = 8.0 Hz, 1H, ArH), 6.93 (d, *J* = 8.4 Hz, 1H, ArH), 6.53 (s, 1H, ArH), 5.82 (s, 1H, ArH), 4.23 (q, *J* = 6.9 Hz, 2H, $C\underline{H}_2CH_3$), 3.83 (s, 3H, OCH_3), 3.65 (s, 4H, piperazinyl), 2.39 (s, 4H, piperazinyl), 2.26 (s, 3H, CH_3), 1.26 (t, *J* = 6.8 Hz, 3H, $CH_2C\underline{H}_3$). HRMS (ESI) for $C_{33}H_{33}N_5O_4$ $[M + H]^+$, calcd: 564.2605, found: 564.2611.

4.1.12.11. *Methyl (Z)-3-(((3-((dimethylamino)methyl)-1H-indol-5-yl)amino)(phenyl)methylene)-2-oxoindoline-6-carboxylate (**A11**).* Yellow solid. Yield: 50%. Mp: 241.2–244.3 °C. ^{1}H NMR (400 MHz, DMSO-d_6) δ 12.35 (s, 1H, NH), 11.13 (s, 1H, NH), 10.92 (s, 1H, NH), 7.54–7.44 (m, 5H, ArH), 7.43 (d, *J* = 1.1 Hz, 1H, ArH), 7.30 (s, 1H, ArH), 7.25–7.15 (m, 3H, ArH), 6.77 (dd, *J* = 8.7, 1.4 Hz, 1H, ArH), 5.78 (d, *J* = 8.2 Hz, 1H, ArH), 3.77

(s, 3H, OCH_3), 3.64 (s, 2H, CH_2), 2.20 (s, 6H, CH_3). ^{13}C NMR (101 MHz, DMSO-d_6) δ 170.71, 166.99, 160.56, 136.10, 134.42, 132.94, 130.39, 129.96, 129.92, 129.66, 128.90, 127.94, 127.54, 127.48, 123.65, 121.76, 118.96, 117.20, 115.04, 112.18, 109.80, 96.32, 56.49, 53.57, 52.20, 44.22, 19.03. HRMS (ESI) for $C_{28}H_{26}N_4O_3$ [M + H]$^+$, calcd: 467.2078, found: 467.2085.

4.1.12.12. *Methyl (Z)-3-(((3-((dimethylamino)methyl)-1-methyl-1H-indol-5-yl)amino)(phenyl)methylene)-2-oxoindoline-6-carboxylate (**A12**).* Yellow solid. Yield: 50%. Mp: 199.5–203.0 °C. ^1H NMR (400 MHz, DMSO-d_6) δ 12.32 (s, 1H, NH), 10.92 (s, 1H, NH), 7.46 (m, 8H, ArH), 7.31 (d, *J* = 8.7 Hz, 1H, ArH), 7.18 (dd, *J* = 8.3, 1.1 Hz, 1H, ArH), 6.85 (dd, *J* = 8.8, 1.4 Hz, 1H, ArH), 5.79 (d, *J* = 8.2 Hz, 1H, ArH), 4.08 (s, 2H, CH_2), 3.77 (s, 3H, OCH_3), 3.74 (s, 3H, CH_3), 2.47 (s, 6H, CH_3). HRMS (ESI) for $C_{28}H_{26}N_4O_3$ [M + H]$^+$, calcd: 481.2234, found: 481.2241.

4.1.12.13. *Methyl (Z)-3-(((3-((dimethylamino)methyl)-1-ethyl-1H-indol-5-yl)amino)(phenyl)methylene)-2-oxoindoline-6-carboxylate (**A13**).* Yellow solid. Yield: 50%. Mp: 233.3–236.1 °C. ^1H NMR (400 MHz, DMSO-d_6) δ 12.38 (s, 1H, NH), 10.91 (s, 1H, NH), 7.51 (ddd, *J* = 12.0, 10.1, 5.9 Hz, 5H, ArH), 7.42 (d, *J* = 0.7 Hz, 1H, ArH), 7.31–7.22 (m, 2H, ArH), 7.17 (dd, *J* = 8.3, 1.3 Hz, 1H, ArH), 7.11 (d, *J* = 1.2 Hz, 1H, ArH), 6.79 (dd, *J* = 8.7, 1.8 Hz, 1H, ArH), 5.76 (d, *J* = 8.2 Hz, 1H, ArH), 4.08 (q, *J* = 7.1 Hz, 2H, $C\underline{H}_2CH_3$),3.77(s, 3H, OCH_3), 3.28 (s, 2H, CH_2), 2.04 (s, 6H, CH_3), 1.29 (t, *J* = 7.2 Hz, 3H, $CH_2C\underline{H}_3$). ^{13}C NMR (101 MHz, DMSO-d_6) δ 170.69, 166.99, 160.30, 136.09, 133.93, 132.97, 130.45, 129.93, 129.83, 129.75, 128.88, 128.84, 128.33, 123.62, 121.79, 118.40, 117.21, 114.97, 111.44, 110.38, 109.79, 96.39, 54.24, 52.19, 45.17, 15.85. HRMS (ESI) for $C_{30}H_{30}N_4O_3$ [M + H]$^+$, calcd: 495.2391, found: 495.2386.

4.1.12.14. *Methyl (Z)-3-(((3-((dimethylamino)methyl)-1-isopropyl-1H-indol-5-yl)amino)(phenyl)methylene)-2-oxoindoline-6-carboxylate (**A14**).* Yellow solid. Yield: 50%. Mp: 219.9–222.0 °C. ^1H NMR (400 MHz, DMSO-d_6) δ 12.39 (s, 1H, NH), 10.93 (s, 1H, NH), 7.53 (d, *J* = 7.1 Hz, 3H, ArH), 7.48 (dd, *J* = 7.4, 1.4 Hz, 2H, ArH), 7.43 (d, *J* = 0.8 Hz, 1H, ArH), 7.35 (s, 1H, ArH), 7.32 (d, *J* = 8.8 Hz, 1H, ArH), 7.18 (dd, *J* = 8.2, 1.2 Hz, 1H, ArH), 7.12 (d, *J* = 0.6 Hz, 1H, ArH), 6.78 (dd, *J* = 8.7, 1.8 Hz, 1H, ArH), 5.76 (d, *J* = 8.2 Hz, 1H, ArH), 4.63 (dt, *J* = 13.3, 6.7 Hz, 1H, $C\underline{H}(CH_3)_2$), 3.77 (s, 3H, OCH_3), 3.37 (s, 2H, CH_2), 2.06 (s, 6H, CH_3), 1.38 (d, *J* = 6.6 Hz, 6H, $CH(C\underline{H}_3)_2$). ^{13}C NMR (101 MHz, DMSO-d_6) δ 170.69, 166.99, 160.34, 136.11, 133.92, 133.01, 130.47, 129.93, 129.85, 129.73, 129.01, 128.84, 128.45, 123.65, 121.80, 118.53, 117.19, 114.96, 110.85, 110.39, 109.79, 96.41, 55.18, 53.04, 52.69, 52.18, 46.19, 15.84. HRMS (ESI) for $C_{31}H_{32}N_4O_3$ [M + H]$^+$, calcd: 509.2547, found: 509.2554.

4.1.12.15. *Methyl (Z)-3-(((3-((4-methylpiperazin-1-yl)methyl)-1H-indol-5-yl)amino)(phenyl)methylene)-2-oxoindoline-6-carboxylate (**A15**).* Yellow solid. Yield: 50%. Mp: 197.2–201.8 °C. ^1H NMR (400 MHz, DMSO-d_6) δ 12.35 (s, 1H, NH), 11.00 (s, 1H, NH), 10.92 (s, 1H, NH), 7.55–7.45 (m, 5H, ArH), 7.43 (d, *J* = 1.1 Hz, 1H, ArH), 7.18 (d, *J* = 8.7 Hz, 3H, ArH), 7.13 (s, 1H, ArH), 6.77 (dd, *J* = 8.6, 1.8 Hz, 1H, ArH), 5.76 (d, *J* = 8.2 Hz, 1H,

ArH), 3.77 (s, 3H, OCH_3), 3.42 (s, 2H, CH_2), 2.29 (m, 8H, piperazinyl), 2.18 (s, 3H, CH_3). ^{13}C NMR (101 MHz, DMSO-d_6) δ 170.69, 166.99, 160.51, 136.07, 134.44, 133.00, 130.42, 129.95, 129.68, 128.85, 128.07, 126.90, 126.63, 123.59, 121.78, 118.74, 117.16, 114.85, 112.06, 109.78, 99.99, 96.28, 56.49, 54.99, 52.44, 52.19, 45.98. HRMS (ESI) for $C_{31}H_{31}N_5O_3$ $[M + H]^+$, calcd: 522.2500, found: 522.2495.

*4.1.12.16. Methyl (Z)-3-(((1-methyl-3-((4-methylpiperazin-1-yl)methyl)-1H-indol-5-yl)amino)(phenyl)methylene)-2-oxoindoline-6-carboxylate (**A16**).* Yellow solid. Yield: 50%. Mp: 188.7–190.8 °C. ^{1}H NMR (400 MHz, DMSO-d_6) δ 12.36 (s, 1H, NH), 10.92 (s, 1H, NH), 7.50 (tt, *J* = 8.0, 4.0 Hz, 5H, ArH), 7.43 (d, *J* = 1.4 Hz, 1H, ArH), 7.24 (d, *J* = 8.7 Hz, 1H, ArH), 7.20–7.16 (m, 2H, ArH), 7.13 (d, *J* = 1.6 Hz, 1H, ArH), 6.83 (dd, *J* = 8.7, 1.9 Hz, 1H, ArH), 5.77 (d, *J* = 8.2 Hz, 1H, ArH), 3.77 (s, 3H, OCH_3), 3.68 (s, 3H, CH_3), 3.39 (s, 2H, CH_2), 2.42–2.17 (m, 8H, piperazinyl), 2.15 (s, 3H, CH_3). ^{13}C NMR (101 MHz, DMSO-d_6) δ 170.70, 166.99, 160.47, 136.11, 134.89, 132.98, 130.75, 130.45, 129.93, 129.86, 129.69, 128.86, 128.32, 123.66, 121.80, 118.75, 117.20, 115.02, 110.64, 110.40, 109.80, 96.38, 55.16, 52.85, 52.64, 52.18, 46.16, 32.84. HRMS (ESI) for $C_{32}H_{33}N_5O_3$ $[M + H]^+$, calcd: 536.2656, found: 536.2660.

*4.1.12.17. Methyl (Z)-3-(((3-(morpholinomethyl)-1H-indol-5-yl)amino)(phenyl)methylene)-2-oxoindoline-6-carboxylate (**A17**).* Yellow solid. Yield: 50%. Mp: 257.0–259.2 °C. ^{1}H NMR (400 MHz, DMSO-d_6) δ 12.35 (s, 1H, NH), 11.25 (s, 1H, NH), 10.92 (s, 1H, NH), 7.55–7.45 (m, 5H, ArH), 7.43 (s, 1H, ArH), 7.37 (s, 1H, ArH), 7.32 (s, 1H, ArH), 7.21 (d, *J* = 8.6 Hz, 1H, ArH), 7.18 (dd, *J* = 8.3, 1.3 Hz, 1H, ArH), 6.78 (dd, *J* = 8.6, 1.6 Hz, 1H, ArH), 5.77 (d, *J* = 8.2 Hz, 1H, ArH), 3.77 (s, 3H, OCH_3), 3.64 (s, 4H, morpholinyl), 3.17 (s, 2H, CH_2), 2.62 (s, 4H, morpholinyl). ^{13}C NMR (101 MHz, DMSO-d_6) δ 170.71, 166.98, 160.61, 136.14, 134.36, 132.93, 130.44, 130.29, 130.25, 129.88, 129.64, 128.93, 128.02, 123.72, 121.81, 119.38, 119.36, 117.21, 115.01, 112.32, 109.81, 96.41, 65.35, 52.20, 52.05, 49.06. HRMS (ESI) for $C_{30}H_{28}N_4O_4$ $[M + H]^+$, calcd: 509.2183, found: 509.2177.

4.2. Pharmacology

4.2.1. Enzyme activity assay

The enzymatic activities of VEGFR-2 (Carna), VEGFR-3 (Invitrogen), PDGFRα (BPS), PDGFRβ (Carna) and FGFR1 (Carna) were determined using well-established mobility shift assays. The kinase reaction buffer consisted of 50 mM HEPES (pH 7.5), 0.0015% Brij35, 10 mM $MgCl_2$ and 2 mM dithiothreitol. The stop buffer contained 100 mM HEPES (pH 7.5), 0.015% Brij-35, 0.2% Coating Reagent and 50 mM EDTA.

Initially, the test compounds were diluted to 50-fold the highest concentration tested using 100% dimethyl sulfoxide (DMSO). One hundred microliters of this dilution was then transferred to a well of a 96-well plate. Control wells with no compound or no enzyme were prepared by adding 100 μL of 100% DMSO to two empty wells of the same 96-well plate, which was marked as the source plate. Then, 5 μL of the compound solution was transferred from the source plate to a new 96-well plate (the intermediate plate). An additional 45 μL of kinase buffer was added to each

well of the intermediate plate, which was then shaken for 10 min. The assay plate was prepared by transferring 5 μL from each well of the 96-well intermediate plate to a 384-well plate, in duplicates. The prepared enzyme solution, containing the appropriate kinase and kinase buffer, was added to each well of the 384-well assay plate, which was then incubated at room temperature for 10 min prior to the addition of 10 μL peptide solution; this contained a fluorescein amidite-labelled peptide substrate and ATP, in kinase buffer. The mixture was incubated at 28°C for 1 h before adding 25 μL stop buffer. The conversion data were copied from the Caliper program, and the values were used to calculate kinase inhibition values using the following equation: percentage inhibition = (max - conversion)/(max - min) × 100.

4.2.2. Cell viability assay

The viability of HEK293T, A549, HT-29 and MCF-7 cells was determined using an MTT (3-(4,5-dimethylthiazol-2-yl)-2,5-diphenyltetrazolium bromide) assay. These cancer cell lines were cultured in minimum essential medium supplemented with 10% foetal bovine serum.

Approximately 4×10^3 cells were suspended in cell culture medium, plated in a 96-well plate and incubated at 37°C in 5% CO_2 for 24 h. The test compounds were added to the culture medium and incubated for a further 72 h. Fresh MTT was then added to each well at a final concentration of 5 μg/mL, and incubated with the cells at 37°C for 4 h. The formazan crystals in each well were dissolved in 100 μL DMSO, and the absorbance at 492 nm (MTT formazan wavelength) and 630 nm (reference wavelength) was measured by a microplate reader. The reported IC_{50} results represented averages of at least three determinations and were calculated using the Bacus Laboratories Incorporated Slide Scanner (Bliss) software.

4.2.3. Flow cytometric assay

Apoptosis of HUVECs, HT-29 and MCF-7 cells was detected using a flow cytometric assay. Briefly, cells were seeded in 6-well plates and incubated overnight. The following day, cells were treated with different concentrations of compound **A8** for 48 hours. The cells and supernatants were harvested and washed twice with cold PBS and then resuspended in 100μl 1× Binding Buffer. 5 μl of FITC Annexin V and 5 μl PI were added in each tube and the cells were then gently vortexed incubated for 15 min at RT (25°C) in the dark. 400 μl of 1× Binding Buffer then added to each tube. The stained cells were analyzed by a flow cytometer (FACS Calibur; BD).

Conflict of interest

The authors have declared no conflict of interest.

Acknowledgements

This work was supported by grants from the National Natural Science Foundation of China (81502924) and Innovation Training Project of Liaoning Province (201610163013).

References

[1] S.P. Ivy, J.Y. Wick, B.M. Kaufman, Nat. Rev. Clin. Oncol. 6 (2009) 569–579.

[2] N. Ferrara, Nat. Rev. Cancer 2 (2002) 795–803.

[3] F. Musumeci, M. Radi, C. Brullo, S. Schenone, J. Med. Chem. 55 (2012) 10797–10822.

[4] N. Ferrara, A.P. Adamis, Nat. Rev. Drug Discov. 15 (2016) 385–403.
[5] A.P. Hall, S. Ashton, J. Horner, Z. Wilson, J. Reens, G.H.P. Richmond, S.T. Barry, S.R. Wedge, Toxicologic Pathology. 44 (2015) 98–111.
[6] N. Ferrara, Endocr. Rev. 25 (2004) 581–611.
[7] D. Bruce, P.H. Tan, Cell Commun. Adhes. 18 (2011) 85–103.
[8] T.H. Ho, E. Jonasch, Future Oncol. 7 (2011) 1247–1253.
[9] S. Wilhelm, C. Carter, M. Lynch, T. Lowinger, J. Dumas, R.A. Smith, B. Schwartz, R. Simantov, S. Kelley, Nat. Rev. Drug Discovery. 5 (2006) 835–844.
[10] F. Hilberg, G.J. Roth, M. Krssak, S. Kautschitsch, W. Sommergruber, U. Tontsch-Grunt, P. Garin-Chesa, G. Bader, A. Zoephel, J. Quant, A. Heckel, W.J. Rettig, Cancer Res. 68 (2008) 4774–4782.
[11] S. Schenone, C. Brullo, M. Botta, Curr. Med. Chem. 15 (2008) 3113–3132.
[12] R. Roskoski Jr, Biochem. Biophys. Res. Commun. 356 (2007) 323–328.
[13] L. Sun, C. Liang, S. Shirazian, Y. Zhou, T. Miller, J. Cui, J.Y. Fukuda, J-Y. Chu, A. Nematalla, X. Wang, H. Chen, A. Sistla, T.C. Luu, F. Tang, J. Wei, C. Tang, J. Med. Chem. 46 (2003) 1116–1119.
[14] G.J. Roth, A. Heckel, F. Colbatzky, S. Handschuh, J. Kley, T. Lehmann-Lintz, R. Lotz, U. Tontsch-Grunt, R. Walter, F. Hilberg, J. Med. Chem. 52 (2009) 4466–4480.
[15] O. Casanovas, D.J. Hicklin, G. Bergers, D. Hanahan, Cancer cell. 8 (2005) 299–309.
[16] Y. Zhao, M. Jiang, S. Zhou, S. Wu, X. Zhang, L. Ma, K. Zhang, P. Gong, Eur. J. Med. Chem. 96 (2015) 369–380.
[17] M. Qin, S. Yan, L. Wang, H. Zhang, Y. Tian, Y. Zhao, P. Gong, Bioorg. Med. Chem., 25 (2017) 1778–1786.
[18] Y. Hao, Y. Chen, Dyes. Pigments., 129 (2016) 186–190.
[19] Z. Han, X. Liang, Y. Wang, J. Qing, L. Cao, L. Shang, Z. Yin, Eur. J. Med. Chem., 116 (2016) 147–155.
[20] K. Devaraj, C. Sollert, C. Juds, P.J. Gates, L.T. Pilarski, Chem. Commun., 52 (2016) 5868–5871.

Legends

Figure 1. Design strategy of the target compounds.

Figure 2. Effects of compound **A8** on cell apoptosis in HUVECs (top), HT-29 (middle) and MCF-7 (bottom) cells.

Figure 3. Docking model of compound **A8** with VEGFR-2. Left: binding model overlap of compound **A8** (grey) and nintedanib (yellow) in the kinase domain (surface representation). Right: potential interactions between **A8** and VEGFR-2 depicted as a stick model. Dashed lines depict contacts between the inhibitor and selected residues.

Scheme 1. Reagents and conditions: (a) chloroacetyl chloride, pyridine, chlorobenzene, r.t., 1 h, then *p*-toluenesulfonic acid, reflux, 8 h; (b) appropriate amine, DIPEA, CH_2Cl_2, 30 °C, 8–12 h, then H_2, Pd/C, EtOH, r.t., 5 h; (c) methyl (*E*)-3-(methoxy(phenyl)methylene)-2-oxoindoline-6-carboxylate, methanol, reflux, 5–10 h; (d) chloroacetyl chloride, Et_3N, EtOAc, r.t., 30 min, then HOAc, reflux, 20 h.

Scheme 2. Reagents and conditions: (a) appropriate amine, HATU, DIPEA, DMF, r.t., 12 h; (b) borane dimethyl sulphide, THF, reflux, 1 h, then HCl, reflux, 30 min; (c) H_2, Pd/C, EtOH, r.t., 6 h; (d) methyl (*E*)-3-(methoxy(phenyl)methylene)-2-oxoindoline-6-carboxylate, methanol, reflux, 5–10 h; (e) appropriate alkyl halide, NaH, CH_2Cl_2, r.t., 3–6 h; (f) CH_2O, appropriate amine, HOAc, 35 °C, 5–8 h.

Table 1. *In vitro* inhibitory profile of compounds **A1–A6**.

Table 2. *In vitro* inhibitory profile of compounds **A7–A17**.

Table 3. Inhibitory activity of compound **A8** against selected angiokinases.

Table 1. *In vitro* inhibitory profile of compounds **A1–A6**.

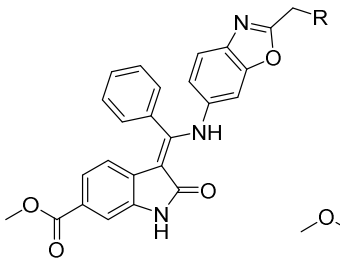

A1 and **A2**

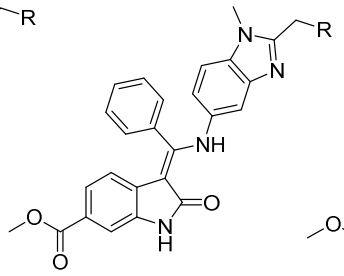

A3 and **A4**

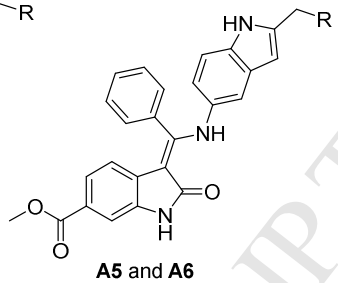

A5 and **A6**

Compound	R	IC_{50} (nM)[a]		IC_{50} (μM)[b]		
		VEGFR-2	PDGFRβ	A549	MCF-7	HT-29
A1		> 1000	>500	>100	NT	NT
A2		79% inhibition[c]	116.2	>100	NT	NT
A3		384.7	45.5	>100	>100	89.87 ± 2.31
A4		257.2	61.0	40.52 ± 1.62	22.54 ± 2.16	0.70 ± 0.12
A5		138.3	NT	16.45 ± 0.88	2.32 ± 0.23	0.98 ± 0.26
A6		106.1	92.7	39.14 ± 1.28	3.27 ± 0.52	0.32 ± 0.03

NT: not tested.

[a] The biological data are generated from at least two independent experiments.

[b] The biological data are generated from at least three independent experiments.

[c] Percent inhibition tested at 1 μM.

Table 2. *In vitro* inhibitory profile of compounds **A7–A17**.

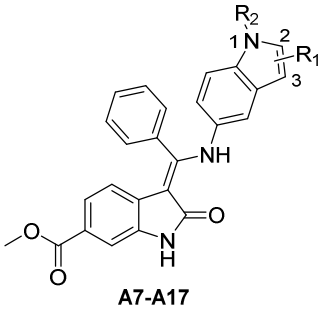

A7-A17

Compound	R1	R2	IC_{50} (nM)[a]		IC_{50} (μM)[b]		
			VEGFR-2	PDGFRβ	A549	MCF-7	HT-29
A7		H	>1000	NT	>100	NT	>100
A8	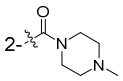	H	69.1	22.0	2.99 ± 0.22	1.56 ± 0.53	1.17 ± 0.18
A9	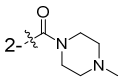	methyl	81.3	44.2	75.19 ± 2.79	NT	1.10 ± 0.02
A10	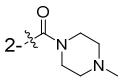	ethyl	104.6	39.0	11.9 ± 1.17	NT	2.19 ± 0.23
A11		H	>1000	60.7	2.27 ± 0.58	3.94 ± 0.76	0.13 ± 0.03
A12		methyl	808.5	64.6	6.01 ± 0.33	2.28 ± 0.50	0.46 ± 0.05
A13		ethyl	431.2	34.3	7.63 ± 0.69	5.53 ± 1.33	6.79 ± 2.07
A14		isopropyl	646.5	49.2	4.32 ± 0.06	5.67 ± 0.78	0.25 ± 0.05
A15	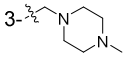	H	59%@1 μM[c]	135.1	7.40 ± 1.32	NT	NT
A16	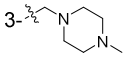	methyl	>1000	91.7	6.15 ± 1.07	4.01 ± 0.68	0.87 ± 0.12
A17	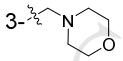	H	NT	241.6	NT	NT	NT
nintedanib			8.5	3.5	22.62 ± 1.57	8.28 ± 0.79	0.83 ± 0.37

NT: not tested.

[a] The biological data are generated from at least two independent experiments.

[b] The biological data are generated from at least three independent experiments.

[c] Percent inhibition tested at 1 μM.

Table 3. Activities of compound **A8** in inhibition of selected angiokinases.

Compound	IC_{50} (nM)[a]				
	VEGFR-2	VEGFR-3	PDGFRα	PDGFRβ	FGFR-1
A8	69.1	18.2	4.4	22.0	1507
nintedanib	8.5	3.2	2.3	3.5	98.2

[a] The biological data are generated from at least two independent experiments.

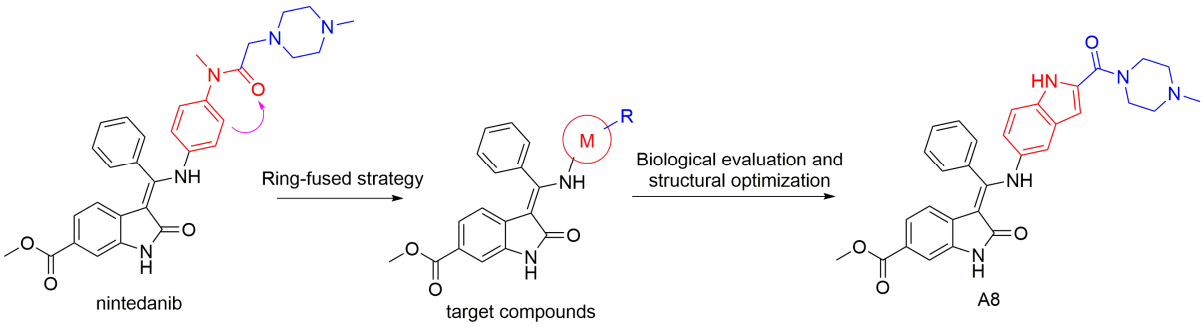

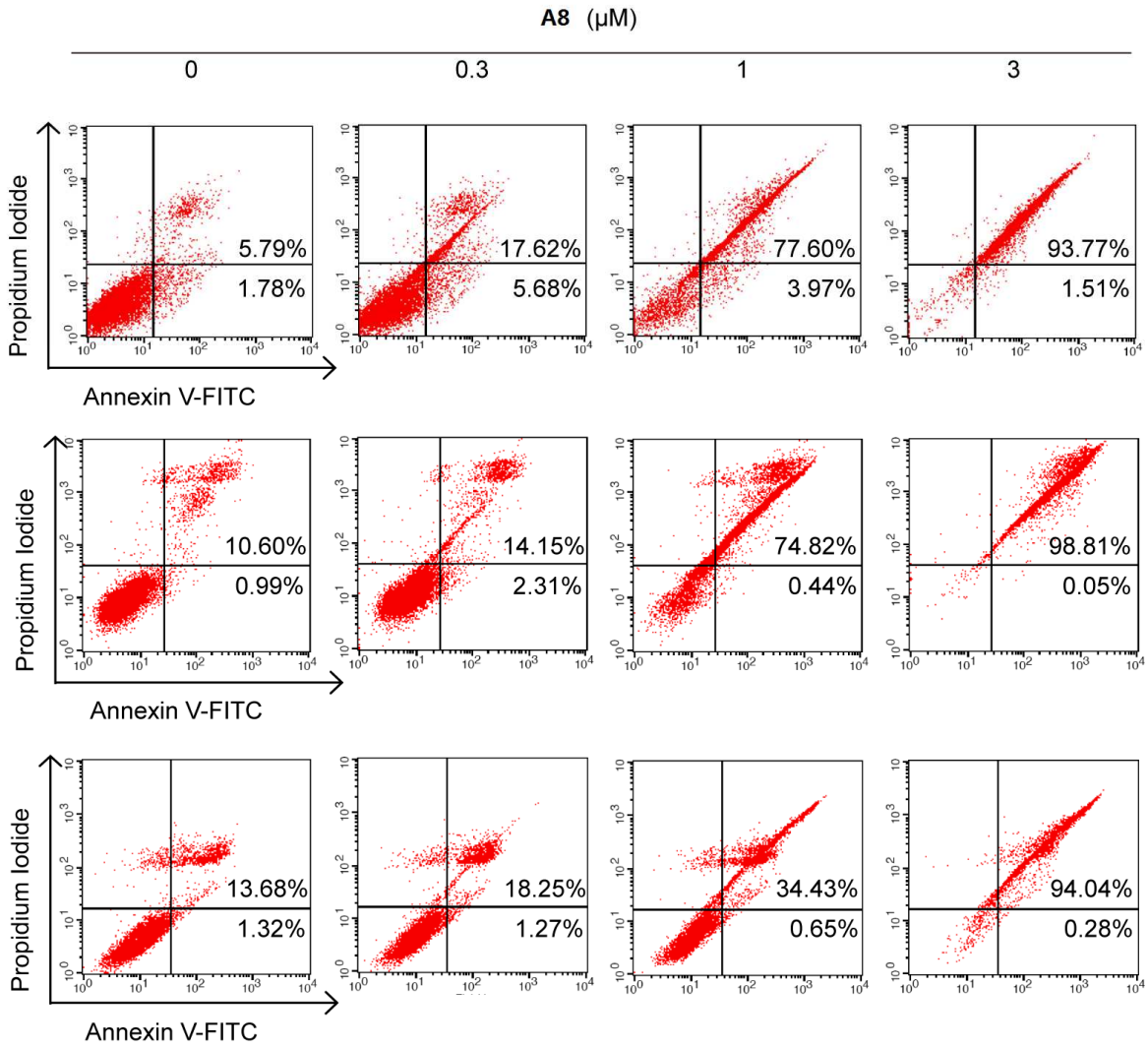
A8 (μM)
0
0.3
1
3
Propidium Iodide
Annexin V-FITC
5.79%
1.78%
17.62%
5.68%
77.60%
3.97%
93.77%
1.51%
10.60%
0.99%
14.15%
2.31%
74.82%
0.44%
98.81%
0.05%
13.68%
1.32%
18.25%
1.27%
34.43%
0.65%
94.04%
0.28%

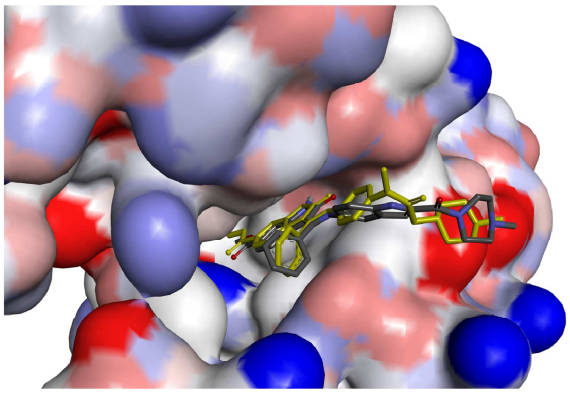

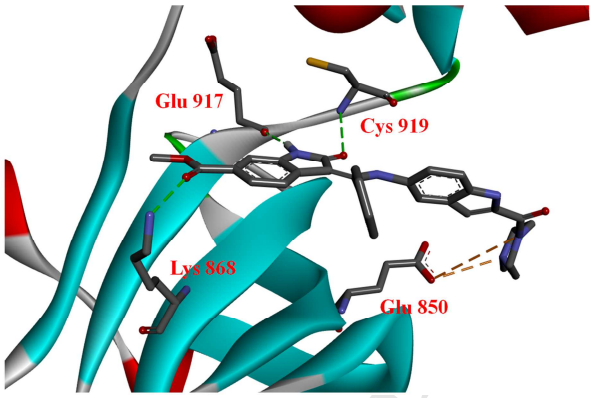

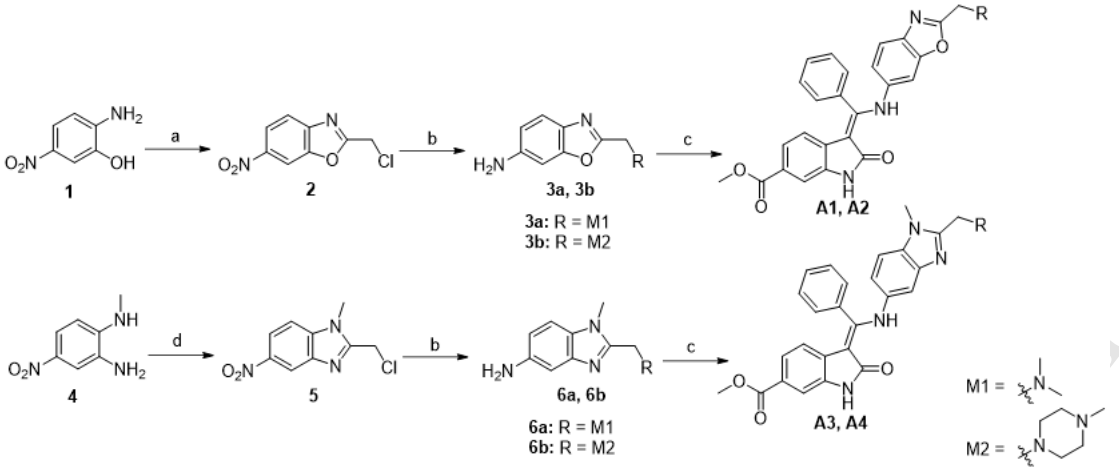

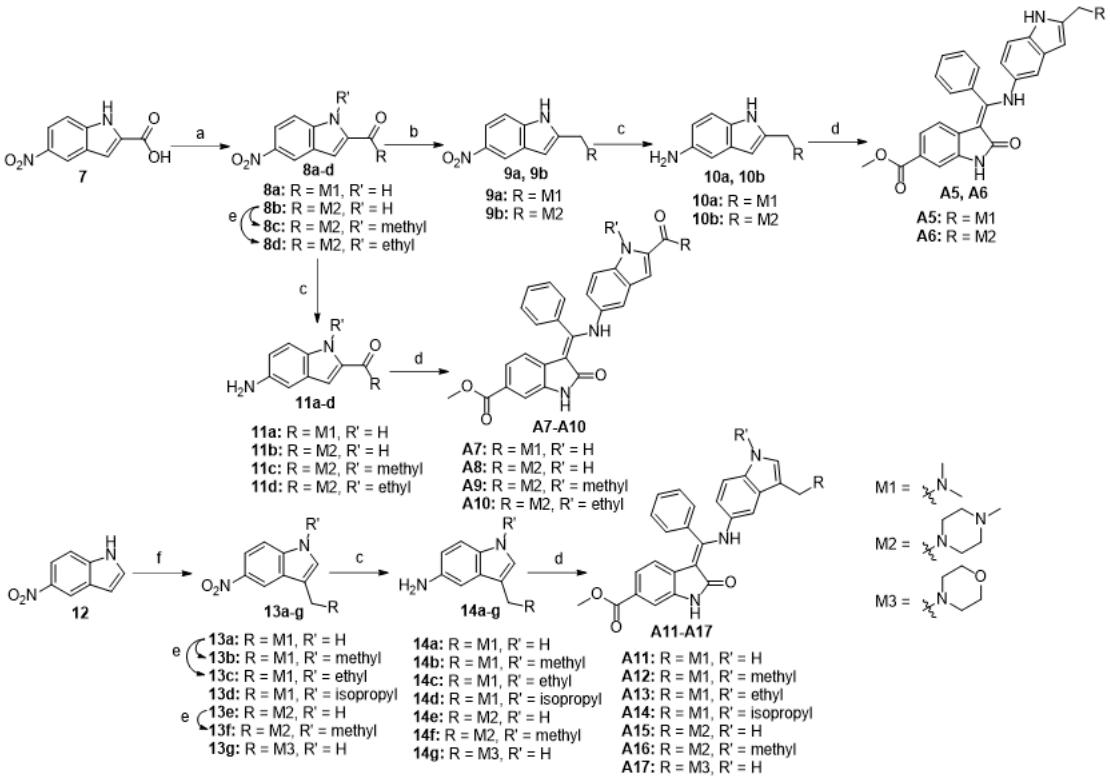

- An indolinone-based compound, **A8**, is identified as a potent angiokinase inhibitor.
- **A8** potently inhibits VEGFR-2, VEGFR-3, PDGFRα and PDGFRβ.
- **A8** induces apoptotic cell death in HUVECs, and HT-29 and MCF-7 cancer cells.